Shape Metrics Based on Elastic Deformations

Matthias Fuchs · Bert Jüttler · Otmar Scherzer · Huaiping Yang

Abstract Deformations of shapes and distances between shapes are an active research topic in computer vision. We propose an energy of infinitesimal deformations of continuous 1- and 2-dimensional shapes that is based on the elastic energy of deformed objects. This energy defines a shape metric which is inherently invariant with respect to Euclidean transformations and yields very natural deformations which preserve details. We compute shortest paths between planar shapes based on elastic deformations and apply our approach to the modeling of 2-dimensional shapes.

Keywords shape space · shape metric · shape modeling · elastic deformation

1 Introduction

This paper is concerned with the problem of quantifying the differences between shapes. This leads to the notion of a *shape space* which is an appropriate representation of shapes and to a *shape metric* on the shape space.

In general, the modeling of both, the shape space and the associated metric, is a challenging task and different approaches lead to diverse models whose usefulness is decided by the application in question. This includes e.g. the statistical analysis of shapes used to regularize the detection or tracking of objects in images and movies. Also the classification of detected outlines

M. Fuchs · O. Scherzer
Dept. of Mathematics, Univ. of Innsbruck, Austria
E-mail: matz.fuchs@uibk.ac.at, otmar.scherzer@uibk.ac.at

O. Scherzer
RICAM, Austrian Acad. of Science, Linz, Austria

B. Jüttler · H. Yang
Inst. of Applied Geometry, Univ. of Linz, Austria
E-mail: bert.juettler@jku.at, yang.huaiping@jku.at

involves statistical methods in shape spaces. Another application is the modeling of shapes. Given two deformed states of one object, the shortest path between the two shapes morphs the first state into the second. The more natural these paths look, the less intermediate steps have to be defined by the designer.

There exists no common shape space or shape metric which satisfies all requirements of the mentioned applications optimally. The suitability of a certain approach depends very much on the demands in a given situation. A property which classifies shape metrics is their invariance with respect to certain geometric transformations. Probably the simplest example is invariance to translations. This means that two shapes are considered to be the same (and thus have distance zero) if they are transformed translationally. In general, translational invariance is considered to be inherent to the notion of "shape".

The situation is less clear when it comes to more general transformations. E.g., if the task is to classify objects in a microscope image it makes obviously no sense to consider the rotation of the shapes as their positions and rotations will be randomly distributed. For the recognition of digits, however, the correct rotation is crucial to distinguish e.g. "6" and "9". On the other hand, the scaling of the digits should not affect the result if one compares image data of different sources. In the above-mentioned example of microscope images, though, the size of the objects might be important. Thus, one favors a translational and rotational invariant metric in the first case but would use a metric invariant to translation and scaling but not to rotation in the second case.

These different invariance properties are reflected in the different approaches to shape spaces and metrics in literature. In principle there exist two, not strictly separated, levels of incorporating invariances. First, the

shape space can be designed in a way such that the shape representation is independent of certain properties. E.g. representing shapes via their tangent vectors removes information about their absolute position, normalizing their perimeter makes them scale invariant. Secondly, it is possible to design metrics which do not consider certain transformations. Then, a shape space might still include translated shapes but the associated shape metric measures the distance between them as zero. This is the approach we chose in this paper where the shape space is only invariant to reparameterizations (a minimal requirement for a shape space) but the shape metric maps any Euclidean transformation to zero.

1.1 Related work

The concept of shape spaces with an associated metric was first developed by Kendall [10]. There, shapes are characterized by labeled points in Euclidean space, so called *land-marks*, and the author investigates Riemannian structures on this space. The drawback of this and related approaches is that the shapes have to be labelled before they can be processed further. On the other hand, the associated spaces are finite dimensional and computationally easy to handle.

More modern works are concerned with continuous shape representations of infinite dimensions. Klassen et al. [12] represent planar curves by their direction and curvature functions. I.e. the shape space is a subspace of the periodic L^2-functions on $[0, 2\pi]$. Such a function corresponds to the angle of the curve tangent in the first and the curvature at a given curve point in the second case. Because the curves are assumed to be parameterized by arclength, this uniquely determines shapes. These representations are invariant to scaling and translation and to scaling, translation and rotation, respectively. The authors impose further properties such as closedness and rotation index via defining functions on the space of curves. This results in a Riemannian manifold embedded in $L^2([0, 2\pi])$ and equipped with the induced metric, i.e. the L^2-metric.

In a similar manner, Mio et al. [18] represent planar curves by the polar coordinates of their tangent vectors. I.e. the angle and the length of the tangent at a curve are smooth functions on the unit interval. They also impose the closure condition via defining functions which results in a shape manifold of infinite dimension. This manifold is Riemannian in virtue of a weighted L^2-metric on the product space of the tangent angles and the tangent lengths. This metric measures the *bending* and *stretching* of curves subject to an infinitesimal de-

formation. The influence of the bending energy versus the stretching energy is controlled by a parameter.

The idea of modeling the boundary curve of a shape as an elastic object is related to Younes [25] but the technical approach there is different from ours. The author considers plane curves which are parameterized by arclength and assumes a group acting transitively on this space. Then, the transformation of one shape into another is represented by a path in this group. Hence, the measurement of distances between shapes is transformed to the problem of defining lengths of paths in the group acting on the shape space. This approach is also presented in a more general manner in Miller and Younes [17]. Invariances of the resulting metric are incorporated via the group action.

The shape metrics presented in Younes [25] and Mio et al. [18] are related to the elastic energy of the boundary curves of the shapes. It is important to note that they do not consider the elastic properties of the domain confined by the shape boundary. This is a significant difference to our approach as noted in Section 1.2.

Michor and Mumford [16] choose smooth embeddings of the unit circle in the plane as shape space and propose a L^2-metric which is regularized by the curvature of the shape boundary. This work is partly motivated by their observation [15] that the standard L^2-metric vanishes on this shape space. An extensive review of metrics on the same shape space can be found in Yezzi and Mennucci [23]. Not only geodesics but gradient flows in general depend on the metric which is chosen on a shape space. How different metrics affect gradient flows of shapes is studied in Sundaramoorthi et al. [20] and Charpiat et al. [5].

A different approach is chosen by Zolésio [26]. In this work the author considers the characteristic functions of measurable sets as shapes and defines *tubes* which are paths between two shapes. Each tube is associated with a time-dependent vector field that prescribes the deformation of the tube. In this formulation lengths of tubes can be defined by imposing norms on the associated function spaces. The idea of defining shape deformations via vector fields defining deformations of the ambient space is related to our approach as explained in Section 3.

Charpiat et al. [4] also consider characteristic functions of shapes and compare norms on these functions to the Hausdorff distance between shapes. In contrast to most of the other papers mentioned here, these metrics are not originally formulated via the energy of infinitesimal deformations. The authors derive smooth approximations of the respective metrics and utilize them to compute geodesics between shapes.

Keeling and Ring [8,9] use the elastic energy of infinitesimal deformations to regularize the optical flow between two images. They assume a time-dependent flow defined on a rectangular image domain which deforms a template image into a reference image. The energy of this flow is computed by integrating the elastic energy of the velocity vector field of the flow over the time. This setup can be used to measure the distance between two shapes if the two images are replaced by the characteristic functions of the shapes. The idea is similar to our approach as presented in Section 3. The main difference is that they integrate the elastic energy of the deformation of the shape *and* the ambient space (i.e. of the whole image domain), whereas we only consider the deformation of the shape.

For the modeling of 2-dimensional shapes, Kilian et al. [11] propose two shape metrics which promote rigid and isometric, respectively, deformations of a discrete boundary mesh. They propose a multi-resolution approach both in time and in space to solve for shortest paths between two shapes.

The present paper is also related to shape optimization. There the goal is to optimize structural parts which are exposed to certain mechanical forces. More mathematically, one seeks a shape which minimizes its elastic energy subject to volume and force constraints. One approach to this problem is to compute the gradient of an objective function and to deform the shape according to the gradient flow. This procedure is similar to the elastic deformation shape modeling in Section 6. In shape optimization however, it is crucial to also consider topological changes of shapes. Allaire et al. [2] combine the traditional shape derivative with the topological gradient which allows for the generation of holes in shapes during the shape deformation.

1.2 Elastic deformations of shapes

In this work we also consider the space of smooth embeddings of the unit circle/sphere modulo reparameterizations and define an energy of infinitesimal deformations of shapes. This allows us to define the length of isotopies (i.e. homotopies taking embedded submanifolds to embedded submanifolds) between shapes and yields a distance measure on the shape space. The energy itself is based on the elastic energy of the shape (i.e. the area inside the shape boundary) caused by an infinitesimal deformation of the shape boundary. Thus, the main characteristics of our approach are:

- The elastic deformation metric takes into account the shape of the actual *object* as opposed to metrics considering only the *boundary curve*.

- It is naturally invariant to rotations and translations.
- The metric applies equally to 1- and 2-dimensional shapes.
- It is formulated for multiply connected shapes.

The first property allows us to distinguish between deforming thin parts of an object (which requires less deformation energy) and thick parts (requiring more energy). This is not possible with any formulation based on local properties of the boundary curve, which is the case for the majority of the approaches cited above.

1.3 Outline

This paper is organized as follows. In the next section we define the elastic deformation energy of infinitesimal deformations of shapes and the corresponding distance measure. Section 3 is devoted to an alternative interpretation of the elastic deformation energy. It is based on vector fields deforming the ambient space of shapes such that the deformation of the metric on the shape is minimal.

The elastic deformation energy is defined via a variational formulation. In Section 4 we prove that minimizers exist and that they are essentially unique. The succeeding section is devoted to the numerical computation of shortest paths between planar shapes. Section 6 considers deformations of shapes in space from a modeling point of view. This means that we do not consider shortest paths between two objects but slowly (i.e. infinitesimally) deform parts of a given object and adapt the rest of the object such that the energy of the infinitesimal deformation is minimal. In the final section we give a short summary and conclude with an outlook.

1.4 Notations and preliminaries

Define $\mathrm{Mat}_n := \mathbb{R}^{n \times n}$, the set of all $n \times n$ matrices. In the following we denote the trace of a matrix by tr, i.e. $\mathrm{tr}\, A = \sum_{i=1}^n A_{ii}$ for $A \in \mathrm{Mat}_n$. The norm $|A|$ is defined as the square root of the sum of the squared components of A, i.e. $|A|^2 = \sum_{i,j=1}^n A_{ij}^2$ and the identity

$$|A|^2 = \mathrm{tr}(A^t A) \tag{1}$$

holds.

In the next section we need the notion of *infinitesimal rotations* in 2- and 3-dimensional space. Formally, infinitesimal rotations constitute the Lie algebra of the respective rotation groups and form linear subspaces of Mat_2 and Mat_3, respectively. These subspaces are the

sets of all skew-symmetric matrices in the respective spaces. They are spanned by

$$\begin{pmatrix} 0 & -1 \\ 1 & 0 \end{pmatrix} \tag{2}$$

in the plane and by

$$\begin{pmatrix} 0 & 0 & 0 \\ 0 & 0 & -1 \\ 0 & 1 & 0 \end{pmatrix}, \begin{pmatrix} 0 & 0 & 1 \\ 0 & 0 & 0 \\ -1 & 0 & 0 \end{pmatrix}, \begin{pmatrix} 0 & -1 & 0 \\ 1 & 0 & 0 \\ 0 & 0 & 0 \end{pmatrix} \tag{3}$$

in space. Any rotation R of $\mathbb{R}^2$ or $\mathbb{R}^3$ can be written as $R = e^{\Psi}$, where Ψ is a linear combination of the matrices (2) or (3), respectively.

Finally, we denote the set of all *infinitesimal Euclidean motions* on $\mathbb{R}^n$, $n = 2, 3$, as

$$M_n := \{A : \mathbb{R}^n \to \mathbb{R}^n : A(x) = a + \Psi x, a \in \mathbb{R}^n,$$
$$\Psi \text{ infinitesimal rotation}\}.$$

2 Elastic Deformation Energy and Distance

In this section we propose an energy of infinitesimal deformations of shapes based on linear elasticity and derive a shape metric from this energy. Moreover, we require the shapes to be smooth and to have a well defined interior area or volume. This naturally leads to smooth embeddings of a parameter domain into its ambient space. Let $n = 1, 2$ and assume $D \subseteq \mathbb{R}^{n+1}$ (the parameter domain) to be a closed, orientable $\mathcal{C}^{\infty}$-manifold of dimension n with no boundary. We denote the embeddings of D in $\mathbb{R}^{n+1}$ by $\mathrm{Emb}(D, \mathbb{R}^{n+1})$, the set of all functions which are $\mathcal{C}^{\infty}$-diffeomorphisms onto their images. The group of all diffeomorphic maps from D onto itself is denoted by $\mathrm{Diff}(D)$. Because several embeddings can represent identical shapes we consider them as equal if a smooth reparameterization can transform one into the other. I.e. we define the space of n-dimensional shapes

$$\mathcal{S}_n = \mathrm{Emb}(D, \mathbb{R}^{n+1}) / \mathrm{Diff}(D), \quad n = 1, 2.$$

For curves or surfaces that bound simply connected domains one can choose $D = S^n$, the n-dimensional unit sphere. This leads to smooth embeddings of the unit circle and the unit sphere, respectively.

Our goal is to define a distance between shapes in $\mathcal{S}_n$. For this purpose we borrow some ideas from Riemannian geometry to compute distances in this space. A Riemannian manifold is a manifold equipped with a Riemannian metric. The Riemannian metric is an inner product on the tangent bundle of the manifold and as such defines angles between tangent vectors. In particular, the length of tangent vectors can be measured with respect to a Riemannian metric.

On manifolds, the distance between two arbitrary points is defined as the infimum of the lengths of all differentiable paths connecting the points. The length of a path is computed by integrating the absolute value of its first derivative along the path, i.e. by integrating its velocity.

The first derivative of a differentiable path on a manifold at a given position is contained in the tangent space at this position. If a representative $r \in \mathrm{Emb}(D, \mathbb{R}^{n+1})$ of shape $a \in \mathcal{S}_n$ is chosen, the tangent space at a is naturally given by $\mathcal{C}^{\infty}(D)$, i.e. by the smooth functions on the parameter domain. The infinitesimal deformation of a prescribed by a tangent vector $f \in \mathcal{C}^{\infty}(D)$ with respect to r in the point $r(\tau)$ is then given by $f(\tau)\mathbf{n}(\tau)$, $\tau \in D$. Here $\mathbf{n}(\tau)$ is the outer unit normal at a in $r(\tau)$.

Using this convention, a differentiable path in $\mathcal{S}_n$ and its velocity are defined as follows:

Definition 1. Let $\gamma : [0, 1] \to \mathcal{S}_n$. Then γ is *differentiable* if there exists $\rho : [0, 1] \to \mathrm{Emb}(D, \mathbb{R}^{n+1})$ satisfying these conditions:

– ρ is differentiable as a function $[0, 1] \to \mathcal{C}^{\infty}(D, \mathbb{R}^{n+1})$, where $\mathcal{C}^{\infty}(D, \mathbb{R}^{n+1})$ is a Banach space with the supremum norm.
– For every $t \in [0, 1]$

$$\gamma(t) = \rho(t) \quad \text{in} \quad \mathcal{S}_n.$$

The derivative $\dot{\gamma} : [0, 1] \to \mathcal{C}^{\infty}(D)$ of γ is given by

$$\dot{\gamma}(t) = \langle \dot{\rho}(t), \mathbf{n}(t) \rangle, \quad 0 \le t \le 1,$$

where $\mathbf{n}(t)$ is the outer unit normal at $\rho(t)$. Then $\dot{\gamma}(t)$ is a tangent vector at $\gamma(t) \in \mathcal{S}_n$ with respect to the representative $\rho(t) \in \mathrm{Emb}(D, \mathbb{R}^{n+1})$.

Note that in this paper $\dot{\gamma}$ and $\partial\gamma/\partial t$ always denote the derivative of a path $\gamma : [0, 1] \to \mathcal{S}_n$ as in Definition 1 and *never* the derivative of the shape parameterization.

To integrate the velocity of a path γ on $\mathcal{S}_n$ the lengths of tangent vectors in $\mathcal{C}^{\infty}(D)$ must be measured. On Riemannian manifolds this is usually done by utilizing the norm induced by the Riemannian metric. In the following, we derive a semi-norm of tangent vectors at $\mathcal{S}_n$. As stated in Remark 14 later on, this semi-norm is induced by a Riemannian pseudo-metric on $\mathcal{S}_n$. In a first step we define the elastic energy of an infinitesimal deformation of a domain Ω, which will later play the role of the shape:

Definition 2. Let $\Omega \subseteq \mathbb{R}^{n+1}$ be a domain with smooth, i.e. $\mathcal{C}^{\infty}$, boundary and assume parameters $\lambda \ge 0$ and $\mu > 0$. Moreover let $\mathbf{u} \in H^1(\Omega, \mathbb{R}^{n+1})$, i.e. $\mathbf{u}$ is a vector

field defined on Ω. Then the *elastic deformation energy of the deformation* $\mathbf{u}$ *on* Ω is given by

$$E(\mathbf{u}) = \int_\Omega \left(\lambda (\operatorname{tr} \mathbf{e}(\mathbf{u}))^2 + 2\mu \operatorname{tr}(\mathbf{e}(\mathbf{u})^t \mathbf{e}(\mathbf{u})) \right) dx \,, \qquad (4)$$

where the components of the *linearized strain tensor* $\mathbf{e}(\mathbf{u})$ are given by

$$e_j^i(\mathbf{u}) = \frac{1}{2}(\partial_j u^i + \partial_i u^j) \,, \quad 1 \le i,j \le n+1 \,. \qquad (5)$$

This defines a map

$$E : H^1(\Omega, \mathbb{R}^{n+1}) \to [0, \infty[\,.$$

In physics, expression (4) is the linear elastic energy of a homogeneous, isotropic material Ω which is displaced by the infinitesimal deformation $\mathbf{u}$. The parameters λ, μ are called the *Lamé parameters* and characterize the elastic properties of the object. It is easy to see that $E(\mathbf{u}) = 0$ if and only if $\mathbf{u}$ is an infinitesimal Euclidean motion, i.e. $\mathbf{u} \in M_{n+1}$.

Using (4) we are able to define the elastic energy of an infinitesimal deformation of shapes in $\mathcal{S}_n$. Such a deformation is given by the displacements of the shape boundary into the directions normal to the boundary. By the definition of $\mathcal{S}_n$ we do not consider displacements tangential to the shape boundary as they correspond to a reparameterization of the shape. Thus, the space of infinitesimal deformations of shapes in $\mathcal{S}_n$ is the space of smooth functions on D, i.e. $\mathcal{C}^\infty(D)$.

Moreover, for shape modeling it turns out to be useful to also consider deformations of parts of the boundary of a domain. The trace operator

$$\operatorname{Tr} : H^1(\Omega) \to H^{1/2}(\partial\Omega)$$

on Sobolev spaces (cf. [1, 5.20 and 7.56]) uniquely extends Sobolev functions on Ω to $\partial\Omega$. This extension to the boundary is canonical in the sense that the trace of continuous functions on Ω corresponds to the their continuous extension to $\partial\Omega$. Let $\Omega \subseteq \mathbb{R}^{n+1}$ be as in Definition 2. We assume a non-empty part $\Gamma \subseteq \partial\Omega$ of the boundary of Ω. Then we define the linear map

$$\operatorname{Tr}_{\mathbf{n}} : H^1(\Omega, \mathbb{R}^{n+1}) \to H^{1/2}(\Gamma), \quad \mathbf{u} \mapsto \langle \operatorname{Tr} \mathbf{u}, \mathbf{n} \rangle \,, \quad (6)$$

where $\mathbf{n}$ denotes the outer unit normal at Ω and $\operatorname{Tr} : H^1(\Omega, \mathbb{R}^{n+1}) \to H^{1/2}(\Gamma, \mathbb{R}^{n+1})$ is the trace operator for vector-valued functions restricted to Γ.

Lemma 3. *The operator* $\operatorname{Tr}_{\mathbf{n}} : H^1(\Omega, \mathbb{R}^{n+1}) \to H^{1/2}(\Gamma)$ *is continuous and surjective, i.e. for every* $f \in H^{1/2}(\Gamma)$ *there exists* $\mathbf{u} \in H^1(\Omega, \mathbb{R}^{n+1})$ *such that*

$$\operatorname{Tr}_{\mathbf{n}}(\mathbf{u}) = f \,.$$

Proof. Since Tr is continuous $H^1(\Omega, \mathbb{R}^{n+1}) \to H^{1/2}(\Gamma, \mathbb{R}^{n+1})$ [1, 7.56] the map $\operatorname{Tr}_{\mathbf{n}}$ is continuous.

Let $f \in H^{1/2}(\Gamma)$. The boundary normal $\mathbf{n} : D \to \mathbb{R}^{n+1}$ is of class $\mathcal{C}^\infty$. As a consequence each component of

$$\mathbf{f} := f\mathbf{n} : \Gamma \to \mathbb{R}^{n+1}$$

lies in $H^{1/2}(\Gamma)$. Moreover, the trace operator $H^1(\Omega, \mathbb{R}^{n+1}) \to H^{1/2}(\Gamma, \mathbb{R}^{n+1})$ is surjective [1, 7.56]. Thus, there exists $\mathbf{u} \in H^1(\Omega, \mathbb{R}^{n+1})$ with $\operatorname{Tr}(\mathbf{u}) = \mathbf{f}$. $\square$

The above considerations are concerned with a domain Ω and a subset Γ of its boundary. In the shape space setting Ω is the interior of a shape. This is reflected in the definition of the elastic deformation energy of a shape:

Definition 4. Assume a shape $a \in \mathcal{S}_n$ and denote

$$\Omega = \text{the open set bounded by the image of } a. \qquad (7)$$

Let $\Gamma \subseteq \partial\Omega$ and $\operatorname{Tr}_{\mathbf{n}}$ be as in (6). Then the *elastic deformation energy* $|f|_{\mathrm{e},a}^2$ *of an infinitesimal boundary deformation* $f \in H^{1/2}(\Gamma)$ is defined by

$$|f|_{\mathrm{e},a}^2 = \inf_{\substack{\mathbf{u} \in H^1(\Omega, \mathbb{R}^{n+1}) \\ \operatorname{Tr}_{\mathbf{n}} \mathbf{u} = f}} E(\mathbf{u}) \,. \qquad (8)$$

In other words, we consider the energies of all infinitesimal deformations of Ω which deform the subset Γ of the boundary in the normal direction as prescribed by f and define $|f|_{\mathrm{e},a}^2$ as the infimum of these energies. We chose the notation $|\cdot|_{\mathrm{e}}^2$ for the elastic energy because its square root plays the role of the semi-norm induced by the Riemannian pseudo-metric in Definition 6.

Remark 5. The variational expression (8) is very similar to the *pure displacement problem* in linear elasticity [6, Section 5.1], where the energy caused by an infinitesimal vector-valued boundary deformation $\mathbf{f} \in H^{1/2}(\Gamma, \mathbb{R}^{n+1})$ is given by

$$\inf_{\substack{\mathbf{u} \in H^1(\Omega, \mathbb{R}^{n+1}) \\ \operatorname{Tr} \mathbf{u} = \mathbf{f}}} E(\mathbf{u}) \,. \qquad (9)$$

The difference between (8) and (9) is that in the latter formulation the infinitesimal deformation $\mathbf{u}$ is completely prescribed on the boundary whereas we only fix its normal components.

Using Definition 4 to measure the magnitude of the velocity of isotopies we can finally define the elastic shape distance on $\mathcal{S}_n$.

Definition 6. Let $a, b \in \mathcal{S}_n$ and $\gamma : [0,1] \to \mathcal{S}_n$ piecewise continuously differentiable such that $\gamma(0) = a$ and $\gamma(1) = b$. The *length* and the *energy* of γ are given by

$$L(\gamma) := \int_0^1 |\dot{\gamma}(t)|_{\mathrm{e},\gamma(t)} \, dt \quad \text{and} \tag{10}$$

$$E(\gamma) := \int_0^1 |\dot{\gamma}(t)|_{\mathrm{e},\gamma(t)}^2 \, dt \,, \tag{11}$$

respectively. Here $\dot{\gamma}(t) : D \to \mathbb{R}$ is the velocity of $\gamma(t)$ normal to $\gamma(t)$, i.e. normal to the shape boundary at the time t, $0 < t < 1$, as in Definition 1. We use the notation $E(\gamma)$ for paths γ exclusively to avoid any confusion with the elastic deformation energy $E(\mathbf{u})$ of an infinitesimal deformation $\mathbf{u}$ as defined in (2). Note that the elastic deformation energy of $\dot{\gamma}$ in (10) and (11) is given by applying the case $\Gamma = \partial\Omega$ in Definition 4.

We define the *elastic deformation distance* $d : \mathcal{S}_n \times \mathcal{S}_n \to [0, \infty[$ by

$$d(a,b) = \inf_{\substack{\gamma(0)=a \\ \gamma(1)=b}} L(\gamma) \,, \tag{12}$$

where $\gamma : [0,1] \to \mathcal{S}_n$ is as above.

Remark 7. Let d be as in Definition 6 and $a, b, c \in \mathcal{S}_n$. Then the following relations hold:

- $d(a,b) = d(b,a)$ and
- $d(a,c) \leq d(a,b) + d(b,c)$.

In other words, the elastic deformation distance is symmetric and satisfies the triangle inequality.

However, the elastic deformation distance between two shapes $a, b \in \mathcal{S}_n$ is zero if a and b only differ by a Euclidean transformation, i.e.

$$d(a,b) = 0 \quad \text{if} \quad a \text{ and } b \text{ differ only by a}$$
$$\text{translation and/or rotation.}$$

In other words, d is only a pseudo-metric on $\mathcal{S}_n$. This is actually the reason why we avoid the notion "metric" altogether and refer to d as a "distance".

Unfortunately, we are not able to show that $d(a,b) > 0$ if $a \neq b$ modulo Euclidean transformations.

In Remark 14 we state that the elastic deformation energy $|\cdot|_\mathrm{e}^2$ is induced by a Riemannian pseudo-metric on $\mathcal{S}_n$. For a path $\gamma : [0,1] \to \mathcal{S}_n$, which connects two shapes $a, b \in \mathcal{S}_n$, this has following two consequences:

- $L(\gamma)$ is invariant to reparameterization of γ.
- Assume that γ is such that its energy $E(\gamma)$ is minimal among all curves connecting a and b. Then $L(\gamma)$ also minimizes the lengths of all paths between a and b and $|\dot{\gamma}|_{\mathrm{e},\gamma}$ is constant along γ.

For the actual computation of distances between shapes and geodesics connecting them several issues remain. The definitions in (8) and (12) are formulated via infima of non-negative sets. This results in well-defined values but does not necessarily imply the existence of minimizing elements. In Section 4 we prove that the infimum of $E(\mathbf{u})$ in (8) is attained by a unique minimizer in $H^1(\Omega, \mathbb{R}^{n+1})$. This enables us to compute $|\cdot|_\mathrm{e}^2$ using a finite element approach to solve the weak formulation of the optimality condition of the variational problem.

The existence of minimal geodesics, i.e. the existence of a γ which minimizes $L(\gamma)$ in (12), is a much harder question. In the finite dimensional setting, one approach to this problem is the Hopf-Rinow Theorem which states the existence of minimal geodesics on a finite dimensional manifold which is complete as a metric space. However in the infinite dimensional case this theorem fails [13]. Due to these difficulties, we computed discrete geodesics as explained in Section 5 but can not provide analytical results concerning their existence.

3 Metric Perturbation

In this section we give an alternative interpretation of the elastic deformation energy based on differential geometry. We derive the perturbation of the metric on a shape which is deformed by an infinitesimal deformation and show that this perturbation is a special case of the elastic deformation energy (8). As mentioned in Remark 10 below, this allows for a generalization to shapes on curved surfaces.

The basic idea is to define a Riemannian metric on $\mathbb{R}^{n+1}$ which reflects the deformation of this space according to a time-dependent flow field. We then compute the perturbation of this metric as the L^2-norm of the time derivative of the metric tensor at the time zero. In the following we give a detailed description of this approach.

Assume a time-dependent vector field $\mathbf{x} : [0, \varepsilon[\to H^1(\mathbb{R}^{n+1}, \mathbb{R}^{n+1})$, $\varepsilon > 0$, which is differentiable at time zero and satisfies $\mathbf{x}(0) = \mathrm{Id}$. This flow can be interpreted as the trajectories of points in $\mathbb{R}^{n+1}$ at a given time. If one considers the space $\mathbb{R}^{n+1}$ as a whole, then $\mathbf{x}(t)$ corresponds to a deformed state of this space at $t > 0$. At the time zero every point is mapped to its initial position, i.e. the space is not deformed, whereas for times $t > 0$ angles and distances between points get distorted. In the following we quantify these distortions in an infinitesimal setting, i.e. we consider the distortion between points at arbitrarily small distances and short times.

First note that we write $D\mathbf{x}(t,p)$ for the *spatial derivative* of $\mathbf{x}(t)$ at a fixed time $0 < t < \varepsilon$ in $p \in \mathbb{R}^{n+1}$.

I.e. the directional derivative of $\mathbf{x}(t)$ into the direction $v \in \mathbb{R}^{n+1}$ is given by $D\mathbf{x}(t,p)(v)$. We choose an orthonormal basis $(v_i)_{1 \leq i \leq n+1}$ of $\mathbb{R}^{n+1}$ and define the *metric tensor* $\mathbf{G_x} = (g_{ij})_{1 \leq i,j \leq n+1}$ in a point $p \in \mathbb{R}^{n+1}$ at the time $t \geq 0$ by

$$g_{ij}(t,p) = \langle D\mathbf{x}(t,p)(v_i), D\mathbf{x}(t,p)(v_j) \rangle$$
$$\text{for} \quad 1 \leq i,j \leq n+1. \quad (13)$$

Note that $\mathbf{G_x}(0,p) = \mathrm{Id}$ for all $p \in \mathbb{R}^{n+1}$. In the next step we define the perturbation of $\mathbf{G_x}$ caused by an infinitesimal deformation of a shape domain.

Definition 8. Assume $a \in \mathcal{S}_n$ and Ω as in (7). Let $\Gamma \subseteq \partial \Omega$ and $\mathrm{Tr}_\mathbf{n}$ as in (6). Then the *metric perturbation* $|f|^2_{\mathrm{m},a}$ induced by an infinitesimal deformation $f \in H^{1/2}(\Gamma, \mathbb{R}^{n+1})$ is defined by

$$|f|^2_{\mathrm{m},a} = \inf_{\mathrm{Tr}_\mathbf{n}\,(\dot{\mathbf{x}}(0)|_\Omega)=f} \int_\Omega \left| \frac{\partial}{\partial t} \mathbf{G_x}(t,p) \right|^2_{t=0} dp, \quad (14)$$

where $\mathbf{x} : [0,\varepsilon[\to H^1(\mathbb{R}^{n+1}, \mathbb{R}^{n+1})$, $\varepsilon > 0$ and $\mathbf{x}(0) = \mathrm{Id}$. Note that $|f|^2_a$ is independent of the choice of $(v_i)_{1 \leq i \leq n+1}$.

In other words, we consider time dependent deformations of the ambient space of the shape a which coincide with the infinitesimal normal deformation f at the time zero. The time derivatives of each such deformation define a metric tensor $\mathbf{G_x}$ and we minimize the L^2-norm of the time derivative of the tensor on Ω. I.e. we penalize temporal changes of the metric inside the shape at the time zero. The next theorem proves that the metric perturbation (14) coincides with the elastic deformation energy (4) in case of Lamé parameters $\lambda = 0$ and $\mu = 2$.

Theorem 9. *Assume a, Γ and f as in Definition 8. Let further be $\lambda = 0$ and $\mu = 2$ in (4). Then*

$$|f|^2_{\mathrm{m},a} = |f|^2_{\mathrm{e},a}.$$

Proof. Consider a vector field $\mathbf{x}$ as in Definition 8 and define $\mathbf{u} \in H^1(\mathbb{R}^{n+1}, \mathbb{R}^{n+1})$ by $\mathbf{u} = \dot{\mathbf{x}}(0)$. Without loss of generality we assume that $(v_i)_{1 \leq i \leq n+1}$ is the standard basis of $\mathbb{R}^{n+1}$. Because $\mathbf{x}(0) = \mathrm{Id}$ the equality

$$\frac{\partial}{\partial t} \langle D\mathbf{x}(t,p)(v_i), D\mathbf{x}(t,p)(v_j) \rangle \Big|_{t=0} =$$
$$\langle D\mathbf{u}(p)(v_i), v_j \rangle + \langle v_i, D\mathbf{u}(p)(v_j) \rangle = \partial_i u^j + \partial_j u^i \quad (15)$$

holds for $1 \leq i,j \leq n+1$ and $p \in \mathbb{R}^{n+1}$. Let $\mathbf{e}(\mathbf{u})$ be as in (5), i.e.

$$e^i_j(\mathbf{u}) = \frac{1}{2}(\partial_j u^i + \partial_i u^j), \quad 1 \leq i,j \leq n+1.$$

Then it follows from (13) and (15) together with the above equation that

$$\left| \frac{\partial}{\partial t} \mathbf{G_x}(t,p) \right|^2_{t=0} = \left| 2\mathbf{e}(\mathbf{u}) \right|^2 = 4 \left| \mathbf{e}(\mathbf{u}) \right|^2.$$

Applying (1) and comparing (4) and (14) concludes the proof. $\square$

Remark 10. The notion of the metric perturbation can easily be extended to shapes on a manifold M. Shapes on M correspond to elements of $\mathrm{Emb}(D, M) / \mathrm{Diff}(D)$. The metric tensor $\mathbf{G_x}$ generalizes to this setting by replacing $D\mathbf{x}$ in (13) by the covariant derivative on M (cf. [3, Chapter VII]).

4 Existence and Uniqueness of Minimizing Deformations

This section is devoted to the existence of unique minimizers of the variational problem which defines the elastic deformation energy in (8). As pointed out in the previous section this problem is very much related to the pure displacement problem in linear elasticity and the following results are a modification of the treatment of this problem in [6, Section 6.4].

First we look at a problem similar to (8) but with homogeneous boundary conditions and non-vanishing source term. We derive a weak formulation of the corresponding PDE and prove existence and uniqueness of solutions of this equation. Moreover, these solutions also solve the original variational problem. Finally, we adapt these results to (8).

We start with the following definitions: Let $\Omega \subseteq \mathbb{R}^{n+1}$ be a domain with smooth boundary, $\emptyset \neq \Gamma \subseteq \partial \Omega$ and $\mathrm{Tr}_\mathbf{n}$ as in (6). Assume $\lambda \geq 0$, $\mu > 0$ and $\mathbf{g} \in H^1(\Omega, \mathbb{R}^{n+1})$. For $\mathbf{u}, \mathbf{v} \in H^1(\Omega, \mathbb{R}^{n+1})$ define

$$B(\mathbf{u}, \mathbf{v}) =$$
$$\int_\Omega \left(\lambda \, \mathrm{tr}\,\mathbf{e}(\mathbf{u}) \, \mathrm{tr}\,\mathbf{e}(\mathbf{v}) + 2\mu \, \mathrm{tr}(\mathbf{e}(\mathbf{u})^t \mathbf{e}(\mathbf{v})) \right) dx, \quad (16)$$

where

$$e^i_j(\mathbf{u}) = \frac{1}{2}(\partial_j u^i + \partial_i u^j), \quad 1 \leq i,j \leq n+1.$$

In the next theorem we are concerned with the task of minimizing a functional defined by (16) subject to homogeneous boundary conditions. We state two different versions of this problem, the variational problem and the weak formulation of the corresponding Euler-Lagrange equations:

Variational formulation: Find $\mathbf{u} \in H^1(\Omega, \mathbb{R}^{n+1})$ such that

$$\begin{cases} \mathrm{Tr_n}\,(\mathbf{u}) = 0 \\ B(\mathbf{u}, \mathbf{u} + 2\mathbf{g}) \leq B(\mathbf{v}, \mathbf{v} + 2\mathbf{g}) \end{cases} \tag{V_{h}}$$

for all $\mathbf{v} \in H^1(\Omega, \mathbb{R}^{n+1})$ with $\mathrm{Tr_n}\,(\mathbf{v}) = 0$.

Weak formulation: Find $\mathbf{u} \in H^1(\Omega, \mathbb{R}^{n+1})$ such that

$$\begin{cases} \mathrm{Tr_n}\,(\mathbf{u}) = 0 \\ B(\mathbf{u}, \boldsymbol{\varphi}) = -B(\mathbf{g}, \boldsymbol{\varphi}) \end{cases} \tag{W_{h}}$$

for all $\boldsymbol{\varphi} \in H^1(\Omega, \mathbb{R}^{n+1})$ with $\mathrm{Tr_n}\,(\boldsymbol{\varphi}) = 0$.

Theorem 11. *A vector field $\mathbf{u} \in H^1(\Omega, \mathbb{R}^{n+1})$ solves (V_{h}) if and only if it solves (W_{h}), i.e. the two problems are equivalent. Moreover, a solution of (V_{h}) and (W_{h}) exists. If $\mathbf{u}, \mathbf{w} \in H^1(\Omega, \mathbb{R}^{n+1})$ solve (V_{h}) and (W_{h}), respectively, then*

$$\mathbf{w} = \mathbf{u} + A \,,$$

where $A \in M_{n+1}$ is an infinitesimal Euclidean motion.

Proof. We start by defining

$$V := \{\mathbf{u} \in H^1(\Omega, \mathbb{R}^{n+1}) : \mathrm{Tr_n}\,(\mathbf{u}) = 0\} \,.$$

First we prove the above claim on a modification of V where we identify deformations which differ only by an infinitesimal Euclidean motion. This allows us to directly apply Korn's inequality on this space. Define

$$\tilde{V} := \{[\mathbf{u}] = \mathbf{u} + M_{n+1} : \mathbf{u} \in V\} \,.$$

Note that this space is not a quotient space of V as M_{n+1} is not a subset of V. However, according to Lemma 12 below, $\tilde{V}$ equipped with the norm

$$\|[\mathbf{u}]\|_{\tilde{V}} = \inf_{\mathbf{u} \in [\mathbf{u}]} \|\mathbf{u}\|_{H^1(\Omega, \mathbb{R}^{n+1})} \quad \text{for} \quad [\mathbf{u}] \in \tilde{V}$$

is a Banach space.

The map

$$\mathbf{e} : \tilde{V} \to L^2(\Omega, \mathrm{Mat}_{n+1}) \,, \quad \mathbf{u} \mapsto \frac{1}{2}(\partial_j u^i + \partial_i u^j)_{1 \leq i,j \leq n+1} \,,$$

is defined on $\tilde{V}$ because it maps infinitesimal Euclidean motions to 0. As a consequence, $B : \tilde{V} \times \tilde{V} \to \mathbb{R}$ is well defined. Hence, by (1),

$$2\mu \|\mathbf{e}([\mathbf{u}])\|_{L^2(\Omega, \mathrm{Mat}_{n+1})}^2 \leq B([\mathbf{u}], [\mathbf{u}]) \quad \text{for} \quad [\mathbf{u}] \in \tilde{V} \,. \tag{17}$$

Korn's inequality [7] states that there exists $C > 0$ such that

$$C\|[\mathbf{u}]\|_{\tilde{V}} \leq \|\mathbf{e}([\mathbf{u}])\|_{L^2(\Omega, \mathrm{Mat}_{n+1})} \quad \text{for} \quad [\mathbf{u}] \in \tilde{V} \,. \tag{18}$$

Combining (17) and (18) yields

$$C'\|[\mathbf{u}]\|_{\tilde{V}}^2 \leq B([\mathbf{u}], [\mathbf{u}]) \quad \text{for} \quad [\mathbf{u}] \in \tilde{V} \tag{19}$$

for some $C' > 0$. We define the linear functional $L : \tilde{V} \to \mathbb{R}$ by

$$L([\boldsymbol{\varphi}]) = B([\mathbf{g}], [\boldsymbol{\varphi}]) \quad \text{for} \quad [\boldsymbol{\varphi}] \in \tilde{V} \,.$$

Note that L is bounded in the sense that $L([\mathbf{u}])/\|[\mathbf{u}]\|$ is bounded for $[\mathbf{u}] \in \tilde{V}$. Inequality (19) means that B is V-elliptic on $\tilde{V}$ in the sense of [6, Theorem 6.3-2]. The same theorem states that there exists a unique solution $[\mathbf{u}] \in \tilde{V}$ of

$$B([\mathbf{u}], [\boldsymbol{\varphi}]) = -L([\boldsymbol{\varphi}]) \quad \text{for all} \quad [\boldsymbol{\varphi}] \in \tilde{V} \tag{20}$$

and that $[\mathbf{u}]$ is the unique solution of

$$B([\mathbf{u}], [\mathbf{u}]) + 2L([\mathbf{u}]) \leq B([\mathbf{v}], [\mathbf{v}]) + 2L([\mathbf{v}])$$
$$\text{for all} \quad [\mathbf{v}] \in \tilde{V} \,. \tag{21}$$

By assumption we can choose $\mathbf{u} \in [\mathbf{u}]$ such that $\mathrm{Tr_n}\,(\mathbf{u}) = 0$. Then $\mathbf{u}$ solves (W_{h}) and (V_{h}).

To prove uniqueness consider two solutions $\mathbf{u}$ and $\mathbf{w}$ of (W_{h}) or (V_{h}). Obviously $[\mathbf{u}]$ and $[\mathbf{w}]$ solve (20) and (21), respectively. Because these problems have unique solutions $[\mathbf{u}] = [\mathbf{w}]$ and therefore $\mathbf{u} = \mathbf{w} + A$ for some $A \in M_{n+1}$. $\qquad\square$

Lemma 12. *The space*

$$\tilde{V} = \{[\mathbf{u}] = \mathbf{u} + M_{n+1} : \mathbf{u} \in H^1(\Omega, \mathbb{R}^{n+1}), \mathrm{Tr_n}\,(\mathbf{u}) = 0\}$$

with norm

$$\|[\mathbf{u}]\|_{\tilde{V}} = \inf_{\mathbf{u} \in [\mathbf{u}]} \|\mathbf{u}\|_{H^1(\Omega, \mathbb{R}^{n+1})} \text{ for } [\mathbf{u}] \in \tilde{V}$$

is a Banach space.

Proof. We first consider the space

$$\bar{H}^1(\Omega, \mathbb{R}^{n+1}) := H^1(\Omega, \mathbb{R}^{n+1})/M_{n+1}$$
$$= \{[\mathbf{u}] = \mathbf{u} + M_{n+1} : \mathbf{u} \in H^1(\Omega, \mathbb{R}^{n+1})\}$$

with norm

$$\|[\mathbf{u}]\|_{\bar{H}^1(\Omega, \mathbb{R}^{n+1})} = \inf_{\mathbf{u} \in [\mathbf{u}]} \|\mathbf{u}\|_{H^1(\Omega, \mathbb{R}^{n+1})}$$
$$\text{for} \quad \mathbf{u} \in \bar{H}^1(\Omega, \mathbb{R}^{n+1}) \,.$$

$\bar{H}^1(\Omega, \mathbb{R}^{n+1})$ is a Banach space as the quotient space of a Banach space and a closed subspace [24, Section I.11].

Moreover $\tilde{V} \subseteq \bar{H}^1(\Omega, \mathbb{R}^{n+1})$. To show the assertion it suffices to prove that $\tilde{V}$ is a closed subspace of $\bar{H}^1(\Omega, \mathbb{R}^{n+1})$.

Consider $[\mathbf{u}_k] \in \tilde{V}$, $k \geq 0$, and $[\mathbf{u}] \in \bar{H}^1(\Omega, \mathbb{R}^{n+1})$, such that

$$\lim_{k \to \infty} [\mathbf{u}_k] = [\mathbf{u}] \quad \text{in} \quad \bar{H}^1(\Omega, \mathbb{R}^{n+1}).$$

Without loss of generality we can assume that

$$\lim_{k \to \infty} \mathbf{u}_k = \mathbf{u} \quad \text{in} \quad H^1(\Omega, \mathbb{R}^{n+1}).$$

Moreover there exists a sequence of infinitesimal Euclidean motions $A_k \in M_{n+1}$, $k \geq 0$, such that

$$\text{Tr}_{\mathbf{n}}(\mathbf{u}_k + A_k) = 0. \tag{22}$$

Because $\text{Tr}_{\mathbf{n}}$ is continuous, this implies that there exists $M \geq 0$ such that

$$\|\text{Tr}_{\mathbf{n}}(A_k)\|_{L^2(\Gamma)} \leq M \quad \text{for} \quad k \geq 0. \tag{23}$$

On the other hand, the map

$$M_{n+1} / \ker \text{Tr}_{\mathbf{n}} \to \text{im}(\text{Tr}_{\mathbf{n}}), \quad A + \ker \text{Tr}_{\mathbf{n}} \mapsto \text{Tr}_{\mathbf{n}} A$$

is a linear bijection of finite dimensional linear spaces. Thus, inequality (23) implies that the sequence $(A_k + \ker \text{Tr}_{\mathbf{n}})_{k \geq 0}$ is bounded in $M_{n+1} / \ker \text{Tr}_{\mathbf{n}}$. Without loss of generality (by selecting an appropriate subsequence) we conclude that there exists $A \in M_{n+1}$ such that

$$\lim_{k \to \infty} (A_k + \ker \text{Tr}_{\mathbf{n}}) = A + \ker \text{Tr}_{\mathbf{n}} \quad \text{in} \quad M_{n+1} / \ker \text{Tr}_{\mathbf{n}}.$$

Moreover, we can choose $(A_k')_{k \geq 0}$ such that

$$A_k' \in A_k + \ker \text{Tr}_{\mathbf{n}} \quad \text{for} \quad k \geq 0.$$

and

$$\lim_{k \to \infty} A_k' = A \quad \text{in} \quad M_{n+1}.$$

Note that by (22) this implies that

$$\text{Tr}_{\mathbf{n}}(\mathbf{u}_k + A_k') = 0.$$

Then, by the continuity of $\text{Tr}_{\mathbf{n}}$, we have

$$\text{Tr}_{\mathbf{n}}(\mathbf{u} + A) = \text{Tr}_{\mathbf{n}}\left(\lim_{k \to \infty}(\mathbf{u}_k + A_k')\right)$$
$$= \lim_{k \to \infty} \text{Tr}_{\mathbf{n}}(\mathbf{u}_k + A_k') = 0.$$

$$\square$$

In a next step we show that the existence of minimizers in (8) follows from Theorem 11. For this purpose we restate the problems (V_{h}) and (W_{h}) without source term but with inhomogeneous boundary conditions:

Variational formulation: Find $\mathbf{u} \in H^1(\Omega, \mathbb{R}^{n+1})$ such that

$$\begin{cases} \text{Tr}_{\mathbf{n}}(\mathbf{u}) = f \\ B(\mathbf{u}, \mathbf{u}) \leq B(\mathbf{v}, \mathbf{v}) \end{cases} \tag{V_{ih}}$$

for all $\mathbf{v} \in H^1(\Omega, \mathbb{R}^{n+1})$ with $\text{Tr}_{\mathbf{n}}(\mathbf{v}) = f$.

Weak formulation: Find $\mathbf{u} \in H^1(\Omega, \mathbb{R}^{n+1})$ such that

$$\begin{cases} \text{Tr}_{\mathbf{n}}(\mathbf{u}) = f \\ B(\mathbf{u}, \boldsymbol{\varphi}) = 0 \end{cases} \tag{W_{ih}}$$

for all $\boldsymbol{\varphi} \in H^1(\Omega, \mathbb{R}^{n+1})$ with $\text{Tr}_{\mathbf{n}}(\boldsymbol{\varphi}) = 0$.

Theorem 13. *A vector field* $\mathbf{u} \in H^1(\Omega, \mathbb{R}^{n+1})$ *solves* (V_{ih}) *if and only if it solves* (W_{ih}), *i.e. the two problems are equivalent. Moreover, a solution of* (V_{ih}) *and* (W_{ih}) *exists. If* $\mathbf{u}, \mathbf{w} \in H^1(\Omega, \mathbb{R}^{n+1})$ *solve* (V_{ih}) *and* (W_{ih}), *respectively, then*

$$\mathbf{w} = \mathbf{u} + A,$$

where $A \in M_{n+1}$ *is an infinitesimal Euclidean motion.*

Proof. According to Lemma 3 there exists $\mathbf{g} \in H^1(\Omega, \mathbb{R}^{n+1})$ such that

$$\text{Tr}_{\mathbf{n}}(\mathbf{g}) = f.$$

By Theorem 11 there exists $\mathbf{u}' \in H^1(\Omega, \mathbb{R}^{n+1})$ which, for $\mathbf{g}$ as above, solves (W_{h}) and (V_{h}), respectively. Then $\mathbf{u} = \mathbf{u}' + \mathbf{g}$ satisfies $\text{Tr}_{\mathbf{n}}(\mathbf{u}) = f$ and further solves (W_{ih}) and (V_{ih}), respectively.

Moreover, assume that $\mathbf{w} \in H^1(\Omega, \mathbb{R}^{n+1})$ solves (W_{ih}) and (V_{ih}), respectively. Then $\mathbf{w}' := \mathbf{w} - \mathbf{g}$ satisfies $\text{Tr}_{\mathbf{n}}(\mathbf{w}') = 0$ and further solves (W_{h}) and (V_{h}), respectively. Thus, $\mathbf{u}'$ and $\mathbf{w}'$ differ only by an infinitesimal Euclidean motion and $\mathbf{u} - \mathbf{w} = \mathbf{u}' - \mathbf{w}' \in M_{n+1}$. $\square$

Remark 14. The elastic deformation energy is induced by a Riemannian pseudo-metric on $\mathcal{S}_n$. Let $a \in \mathcal{S}_n$, Ω and Γ be as in Definition 4 and define the inner product $\langle \cdot, \cdot \rangle_a$ by

$$\langle f, g \rangle_a = B(\mathbf{u}, \mathbf{v}),$$
$$\text{where} \quad \begin{cases} E(\mathbf{u}) = |f|_{\text{e},a}^2 \text{ and } \text{Tr}_{\mathbf{n}}(\mathbf{u}) = f, \\ E(\mathbf{v}) = |g|_{\text{e},a}^2 \text{ and } \text{Tr}_{\mathbf{n}}(\mathbf{v}) = g. \end{cases} \tag{24}$$

for $f, g \in H^{1/2}(\Gamma)$. By Theorem 13 the inner product (24) is well-defined and linear in each component. Moreover it is symmetric and

$$\langle f, f \rangle_a = |f|_{\text{e},a}^2$$

holds for $f \in H^{1/2}(\Gamma)$.

Remark 15. Note that Theorem 13 not only states that the infimum in (8) is attained in $H^1(\Omega, \mathbb{R}^{n+1})$, i.e. a solution of (V_{ih}) exists, but also that it is uniquely (up to infinitesimal Euclidean motions) determined by the weak formulation (W_{ih}). In the next section, a finite element approach to solve (W_{ih}) is derived.

5 Computation of the Elastic Deformation Energy and Shortest Paths in the Plane

The evaluation of the elastic deformation energy (8) requires to numerically solve for the displacement field $\mathbf{u}$ in the problems (V_{ih}) and (W_{ih}), respectively. The first part of this section is devoted to the computation of $\mathbf{u}$ using a finite element approach.

The second part considers the computation of a numerical approximation of the elastic deformation distance as defined in Definition 6. This is done by computing a sequence of discretized paths minizing $E(\gamma)$ as in (11) using a Quasi-Newton method.

In Section 5.3 we demonstrate the capabilities of this approach. Finally, we compare paths approximating the elastic deformation distance to geodesics with respect to other metrics on $\mathcal{S}_n$. In this section we restrict ourselves to the case of planar shapes, i.e. $n = 1$.

5.1 Computation of the elastic deformation energy

Consider a shape $a \in \mathcal{S}_1$, the domain $\Omega \subseteq \mathbb{R}^2$ defined by a and a subset $\Gamma \subseteq \partial \Omega$ of the shape as in Theorem 11. Furthermore, let $f \in H^{1/2}(\partial \Omega)$ and $\lambda \geq 0$, $\mu > 0$ be as in Theorem 13.

We want to solve (W_{ih}) on a finite dimensional subspace of $H^1(\Omega, \mathbb{R}^{n+1})$. First assume that Ω is a polygon defined by points $\{q_1, \ldots, q_M\} \subseteq \mathbb{R}^2$, i.e. we consider discretizations of shapes. For a fixed $h > 0$ we triangulate the discretized shape such that the maximal area of each triangle is smaller than h and that boundary nodes of the triangulation coincide with the boundary discretization $q_1, \ldots, q_M$. Denote the nodes of the triangulation as $\{p_1, \ldots, p_K\} \in \mathbb{R}^2$. Then

$$\{q_1, \ldots, q_M\} \subseteq \{p_1, \ldots, p_K\}\,.$$

For $1 \leq k \leq K$, let φ_k be the unique continuous function which is affine on each triangle of the triangulation and which satisfies

$$\varphi_k(p_\ell) = \begin{cases} 1 & k = \ell\,, \\ 0 & k \neq \ell\,. \end{cases}$$

In other words, $\varphi_1, \ldots, \varphi_K$ is the family of linear splines with nodes $\{p_1, \ldots, p_K\}$.

For $1 \leq k \leq K$ define the vector-valued test functions

$$\boldsymbol{\varphi}_k^1 := (\varphi_k, 0)^t \quad \text{and} \quad \boldsymbol{\varphi}_k^2 := (0, \varphi_k)^t\,,$$

and let

$$W := {}_{\mathbb{R}}\langle \boldsymbol{\varphi}_k^1, \boldsymbol{\varphi}_k^2 : 1 \leq k \leq K \rangle\,,$$

be the $\mathbb{R}$-linear hull of all test functions, i.e. the set of all vector-valued, piecewise linear functions on the triangulation defined by the nodes $\{p_1, \ldots, p_K\}$.

Assume now that the boundary deformation f lies in the trace space of W, i.e.

$$f = \text{Tr}_{\mathbf{n}}\, \mathbf{g} \quad \text{for some} \quad \mathbf{g} \in W\,.$$

Because all the results in Section 4 are valid for W instead of $H^1(\Omega, \mathbb{R}^2)$, a solution of (V_{ih}) in the space W exists and the solution is unique in the sense of Theorem 13.

Let $\mathbf{u} \in W$ be a solution of (V_{ih}). By Definitions 2 and 4 and by comparison of (4) and (16), the equality

$$|f|_{\text{e},a}^2 = B(\mathbf{u}, \mathbf{u}) \tag{25}$$

holds. Then

$$B(\mathbf{u}, \boldsymbol{\varphi}_k^i) = 0$$
$$\text{for} \quad p_k \notin \Gamma\,, \ 1 \leq k \leq K\,, \ 1 \leq i \leq 2\,, \tag{26}$$

i.e. $\mathbf{u}$ satisfies the weak formulation (W_{ih}) for every test function without support on Γ.

For every boundary discretization point $p_k \in \partial \Omega$, $1 \leq k \leq K$, (i.e. for every p_k such that $p_k = q_m$ for some $1 \leq m \leq M$) we define

$$\boldsymbol{\varphi}_k^{\mathbf{t}} = \varphi_k \mathbf{t}(p_k)\,,$$

where $\mathbf{t}(p_k)$ is the outer unit normal at Ω in the boundary point p_k rotated by $\pi/2$. This implies that $\mathbf{t}(p_k)$ is tangential at $\partial \Omega$ in p_k.

In the next section, $\partial \Omega$ is represented as a continuously differentiable B-spline curve and the p_k are points on this curve. Thus, we can compute $\mathbf{t}(p_k)$ at every point on the curve. The test function $\boldsymbol{\varphi}_k^{\mathbf{t}}$ then satisfies $\text{Tr}_{\mathbf{n}}(\boldsymbol{\varphi}_k^{\mathbf{t}})(p_k) = 0$, and, under the simplifying assumption that the boundary normal is locally constant,

$$B(\mathbf{u}, \boldsymbol{\varphi}_k^{\mathbf{t}}) = 0 \quad \text{for} \quad p_k \in \Gamma\,, \ 1 \leq k \leq K\,, \tag{27}$$

holds. By "locally constant" we mean that

$$\text{Tr}_{\mathbf{n}}(\boldsymbol{\varphi}_k^{\mathbf{t}}) = \varphi_k \langle \mathbf{t}(p_k), \mathbf{n} \rangle \approx 0 \quad \text{on} \quad \partial \Omega\,.$$

If $\partial \Omega$ is sampled densely enough this condition is approximately met. Moreover,

$$\int_\Gamma \text{Tr}_{\mathbf{n}}(\mathbf{u}) \varphi^k\, d\tau = \int_\Gamma f \varphi^k\, d\tau$$
$$\text{for} \quad p_k \in \Gamma\,, \ 1 \leq k \leq K\,. \tag{28}$$

Now assume that

$$\mathbf{u} = \sum_{k=1}^K \varphi_k (u_1^k, u_2^k)^t \in W \tag{29}$$

for coefficients $u_1^k, u_2^k \in \mathbb{R}$, $1 \leq k \leq K$. If m_1 is the number of boundary vertices in Γ then equations (26), (27) and (28) yield $2(K-m_1)+m_1+m_1$ linear equations in the unknown coefficients $(u_1^k, u_2^k)_{1 \leq k \leq K}$. Thus, (26), (27) and (28) define a system of linear equations

$$\underline{M}\,\underline{u} = \underline{f}, \tag{30}$$

where $\underline{M} \in \mathrm{Mat}_{2K}$, $\underline{f} \in \mathbb{R}^{2K}$, and $\underline{u} \in \mathbb{R}^{2K}$ is the column vector of the coefficients $(u_1^k, u_2^k)_{1 \leq k \leq K}$. In the implementation, the integrals over the domain Ω were computed by evaluating the respective function in the barycenter of each triangular element, i.e. the integral of a function f over a triangle T given by points $p_{k_1}, p_{k_2}, p_{k_3}$ was approximated by

$$\int_T f\,dx \approx f((p_{k_1} + p_{k_2} + p_{k_3})/3)\,.$$

The integration along the boundary $\partial\Omega$ is done by Gaussian quadrature with two nodes on each boundary edge of the triangulation, i.e.

$$\int_b f\,d\tau \approx \frac{1}{2}\big(f(b(-\sqrt{1/3})) + f(b(\sqrt{1/3}))\big)\,,$$

where $b : [-1,1] \to \mathbb{R}^2$ is the affine parameterization of a boundary edge.

Having obtained a solution $\mathbf{u}$ by solving (30), we compute the elastic energy $|f|_{\mathrm{e},\gamma}^2$ by evaluating the integral on the right hand side of (25). Again, we use barycentric integration on each triangle in T. Note that (25) is an integral of a quadric in $\partial_j u^i$, $1 \leq i, j \leq 2$ over Ω. As such it can be transformed into a boundary integral along $\partial\Omega$ by virtue of the divergence theorem.

The linear equation (30) is sparse and, because of the discretization of the boundary conditions as in (27) and (28), not symmetric. Note however that (W_{h}) is a symmetric problem and that it can be symmetrically discretized if the representation of $\mathbf{u}$ in (29) is adapted to the domain Ω. For implementational reasons we chose the presented version.

Moreover, remember that solutions of (V_{ih}) are unique only up to infinitesimal Euclidean transformations. For most domains Ω this has no consequences because adding an infinitesimal Euclidean transformation to a solution $\mathbf{u}$ of (V_{ih}) would violate the boundary conditions prescribed on Γ. In these cases (30) has a unique solution and we were able to solve the system of linear equations via LU decomposition of $\underline{M}$.

One notable exception, though, is the disc in the plane. Any infinitesimal rotation around the center of the disc does not change the energy of an underlying deformation and leaves the boundary conditions unaffected:

maximal triangle area	# boundary discret. points	energy	
		translation	offset
1.0000	64	8.38e-04	33.423
0.2500	128	6.31e-05	33.355
0.0625	256	4.35e-06	33.336

Table 1 The elastic deformation energy of the boundary deformations in Figure 1 for different discretizations of the shape domain. The *first two* columns refer to the maximal area of the triangles in the FE mesh and to the number of boundary discretization points on the shape, respectively. The *third* and the *fourth* column give the elastic deformation energy for the *upper* and *lower* boundary deformations in Figure 1, respectively.

Example 16. Assume $\Omega = B_1(0) \subseteq \mathbb{R}^2$ and $\emptyset \neq \Gamma \subseteq \partial\Omega = S^1$. For a function $f \in L^2(\Gamma, \mathbb{R})$ let $\mathbf{u}$ be a solution of (V_{ih}). Let $A \in M_2$ be an infinitesimal rotation around 0. Then $\mathbf{u} + A$ solves (V_{ih}). This means that we must expect (30) to be numerically underdetermined. Indeed, it turns out to be impossible to solve (30) in a stable way in this example. Hence, we further restrict possible solutions by seeking a minimum-norm solution of the coefficient vector $\underline{u}$:

$$\begin{cases} \underline{M}\,\underline{u} = \underline{f}, & \text{and} \\ |\underline{u}| \leq |\underline{v}| & \text{for} \quad \underline{M}\,\underline{v} = \underline{f} \end{cases} \tag{31}$$

Using Lagrangian multipliers, this leads to the problem of computing a stationary point of

$$|\underline{u}|^2 + \Lambda^t(\underline{M}\,\underline{u} - \underline{f})\,, \tag{32}$$

where $\Lambda \in \mathbb{R}^{2K}$. Differentiating (32) yields the following system of linear equations for $\underline{u}$ and Λ:

$$\begin{pmatrix} \underline{M} & 0 \\ 2I_K & \underline{M} \end{pmatrix} \begin{pmatrix} \underline{u} \\ \Lambda \end{pmatrix} = \begin{pmatrix} \underline{f} \\ 0 \end{pmatrix} \tag{33}$$

In case (30) is underdetermined, the regularized formulation (32) leads to a unique solution $\underline{u}$ but the system (33) remains underdetermined (being a simple extension of (32)). However, the instability of the problem now affects Λ but not $\underline{u}$. In this example we were able to solve (33) using the *BiCgStab* solver [21].

In Figure 1 we illustrate the vector fields minimizing the elastic deformation energy for two different infinitesimal boundary deformations. The first one corresponds to a translation of the shape and the second one to a constant offset of the shape boundary. Obviously the energy should be zero in the first case. Table 1 shows the computed energies for both cases and their dependency on the discretization of the shape domain.

5.2 Computation of shortest paths

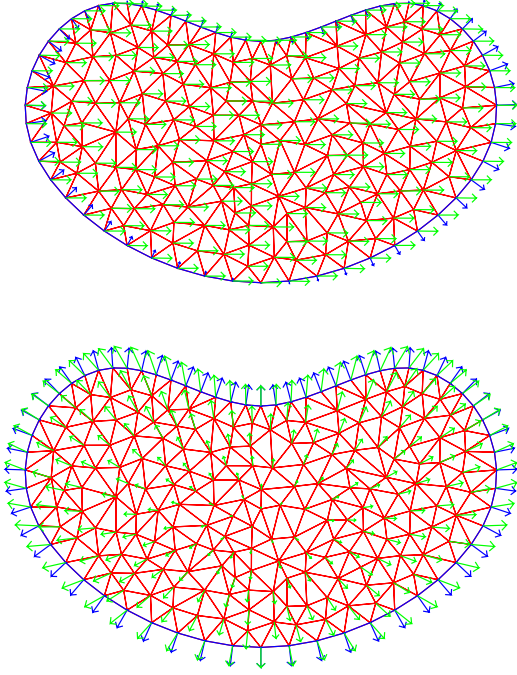This section is concerned with the computation of paths of minimal energy connecting two planar shapes. I.e. for

Fig. 1 Displacement fields (*green*) minimizing the elastic energy (8) of the infinitesimal deformation into normal direction prescribed on the shape boundary (*blue*). In the *top* image the boundary deformation corresponds to a translation of the shape, in the *bottom* image to a boundary offset. The results were obtained for $\mu = 2$ and $\lambda = 0$ in (4).

shapes $a, b \in \mathcal{S}_1$ we compute a discrete path $\bar{\gamma}$ such that $E(\bar{\gamma})$ approximates

$$\inf_{\substack{\gamma(0)=a \\ \gamma(1)=b}} E(\gamma) = \inf_{\substack{\gamma(0)=a \\ \gamma(1)=b}} \int_0^1 |\dot{\gamma}(t)|^2_{\gamma(t)} \, dt \,, \tag{34}$$

for a given norm $|\cdot|_a$, $a \in \mathcal{S}_1$. Naturally we are mainly interested in the case $|\cdot|_a = |\cdot|_{e,a}$ but also minimize (34) with respect to other norms for reasons of comparison.

To minimize (34) we consider $a, b \in \mathcal{S}_1$ to be periodic, cubic B-spline curves determined by $K \geq 4$ control points. We assume the knots of the basis splines to be uniformly distributed on the unit circle. In other words,

$$D = \{p \in \mathbb{R}^2 : |p| = 1\} \,.$$

Moreover, we assume the paths γ in (34) to be discretized in time. I.e. for a discretization level $d \in \mathbb{N}$, a path γ connecting a and b is given by intermediate shapes $\gamma_1, \dots, \gamma_d \in \mathcal{S}_1$ each of which are again cubic B-spline curves with K control points. Denoting $\gamma_0 := a$ and $\gamma_{d+1} := b$, the vectors of the B-spline control points of $\gamma_0, \dots, \gamma_{d+1}$ are called $\mathbf{c}_0, \dots, \mathbf{c}_{d+1}$, respectively. Each $\mathbf{c}_k$, $0 \leq k \leq d+1$, resides in $\mathbb{R}^{2K}$.

The time derivative $\dot{\gamma}$ is then approximated by the discrete derivatives forward and backward in time,

$$\begin{aligned} \dot{\gamma}_k^+ &: D \to \mathbb{R}^2 \,, \ \tau \mapsto \langle \gamma_{k+1}(\tau) - \gamma_k(\tau), \mathbf{n}_k(\tau) \rangle \,, \\ \dot{\gamma}_\ell^- &: D \to \mathbb{R}^2 \,, \ \tau \mapsto \langle \gamma_\ell(\tau) - \gamma_{\ell-1}(\tau), \mathbf{n}_\ell(\tau) \rangle \,, \end{aligned} \tag{35}$$

for $0 \leq k \leq d$ and $1 \leq \ell \leq d+1$. Here $\mathbf{n}_k$ denotes the outer unit normal at γ_k, $0 \leq k \leq d+1$.

Obviously, the discrete time derivatives (35) depend on the parameterization of the respective spline curves. To get a reasonable approximation of $\dot{\gamma}$, the parameterizations of two subsequent curves γ_k and γ_{k+1} must be similar in the sense that $\gamma_k(\tau)$ and $\gamma_{k+1}(\tau)$ are corresponding points for $\tau \in D$. The parameterization of a B-spline curve is determined by its control polygon, i.e. the polygon defined by a coefficient vector $\mathbf{c}_k$, $0 \leq k \leq d+1$. Thus, if the coefficient vectors $\mathbf{c}_0, \dots, \mathbf{c}_{d+1}$ vary smoothly, we expect (35) to be a satisfying discretization of $\dot{\gamma}$. How this was achieved in the examples in this paper is explained below.

For the discretization level d, we define the map $E_d : \mathbb{R}^{2Kd} \to \mathbb{R}$ by

$$(\mathbf{c}_1, \dots, \mathbf{c}_d) \mapsto \frac{1}{d+1} \sum_{k=0}^d \frac{1}{2} \Big(\int_{\gamma_k} |\dot{\gamma}_k^+|^2_{\gamma_k} \, d\tau + \\ \int_{\gamma_{k+1}} |\dot{\gamma}_{k+1}^-|^2_{\gamma_{k+1}} \, d\tau \Big) \,. \tag{36}$$

In other words, E_d approximates the energy of the path defined by $\gamma_0, \dots, \gamma_{d+1}$ by replacing the derivative $\dot{\gamma}$ with symmetric finite differences at the discretization points. The integrals in (36) are computed by a simple equidistant discretization of the curve parameter $\tau \in D$.

We minimize E_d using the L-BFGS method [14] with numerically computed gradients. The resulting coefficient vectors define the approximate shortest path $\bar{\gamma}$. As initial value for the minimization we chose

$$\mathbf{c}_k = (1-t)\mathbf{c}_0 + t\mathbf{c}_{d+1} \,, \quad t = \frac{k}{d+1} \,, \quad 1 \leq k \leq d \,. \tag{37}$$

I.e. the starting sequence of the coefficients $\mathbf{c}_1, \dots, \mathbf{c}_d$ linearly interpolates the control coefficients of the shapes a and b. In our examples this ensures that the parameterizations of the initial discretization $\gamma_1, \dots, \gamma_d$ vary smoothly enough for (35) to approximate $\dot{\gamma}$ well enough.

We experienced in the numerical experiments that this property is preserved during the iterative minimization of E_d. The reason for this behavior is that the minimization process tries to reparameterize $\gamma_1, \dots, \gamma_d$ (by optimizing the respective control polygons $\mathbf{c}_1, \dots, \mathbf{c}_d$) such that E_d is minimal. "Bad" parameterizations, however, usually lead to higher energies of the approximated derivatives (35) and hence to higher values of E_d.
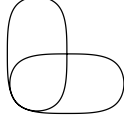
Fig. 2 Initial configuration of two rounded rectangles rotated by $\frac{\pi}{2}$.

The initialization (37) depends on the parameterizations of the start shape a and the end shape b. In other words, the initial correspondence between the shapes $\gamma_0, \ldots, \gamma_{d+1}$ is determined by the parameterizations of a and b. So far, no heuristics for an optimal alignment of a and b have been used. During the minimization of E_d however, the intermediate shapes $\gamma_1, \ldots, \gamma_d$ are potentially reparameterized as illustrated in Figure 4.

As an alternative the approach used in Section 6 later on can be considered. It is independent of the parameterization of the shape.

5.3 Numerical results

All of the following examples are concerned with approximations of shortest path between two given shapes. The paths were computed by minimizing E_d as explained in the previous section. The number of intermediate shapes was $d = 4$.

For all presented results we chose $\mu = 2$ and $\lambda = 0$ in (4). The triangles in the images concerning the elastic deformation distance are the triangulation and the boundary discretization of the start shape used for the finite element implementation of the elastic deformation energy. Note that a separate triangulation is computed for each intermediate shape.

In Figures 3–6 we moved the computed shapes either horizontally or vertically apart. Originally, the start and end shapes lie on top of each other and are not translated.

The first two examples illustrate the capability of the discretization (36) to produce consistent results. In Figure 2 the initial configuration of two shapes is illustrated. Figure 3 shows the linear interpolation (37) of the two shapes and the result of minimizing E_d. In other words, departing from the linear interpolation the minimization process converges to a counter-clockwise rotation of the shape. Obviously the elastic deformation distance between these two shapes is zero and any other path which moves the start shape to the end shape by means of Euclidean motions is also a minimal one.

The second example in Figure 4 is concerned with identical start and end shapes but their parameteriza-
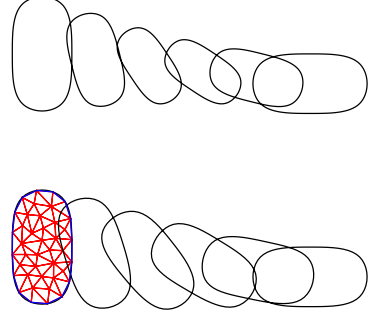

Fig. 3 *Top*: Linear interpolation (37) of the B-spline control points of the shapes in Figure 2. *Bottom*: A shortest path with respect to the elastic deformation energy (8) connecting the shapes in Figure 2. The path was obtained by minimizing E_d as defined in (36).
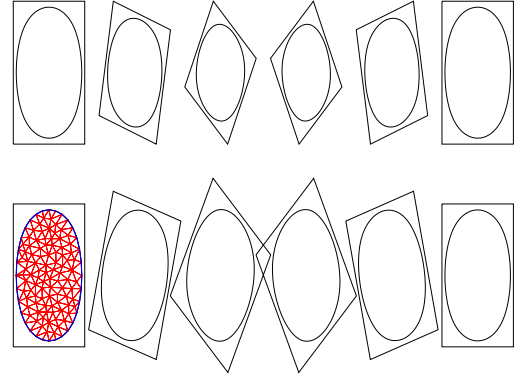

Fig. 4 Two paths connecting identical start and end shapes. Each shape is surrounded by its B-spline control polygon. The numeration of the control points of the *right* shape is shifted by one. On the *top*, equally numbered control points are linearly interpolated which leads to a deformation of the control polygon and the shape. On the *bottom* a shortest path with respect to the elastic deformation energy is shown. The shape is only deformed in tangential direction, i.e. it is reparameterized.

tion is different. From the linear interpolation of the initial shapes the minimization procedure converges to a reparameterization of the start to the end shape. This illustrates that the proposed algorithm is able to correctly reparameterize shapes provided the initial value is well-chosen. Again, any other reparameterization of the start shape to the end shape is also a minimal one.

In the following we compute shortest paths for the elastic deformation energy and compare them to the corresponding results for the L^2-energy and the regularized L^2-energy as proposed by Michor and Mumford [16]. The L^2-energy maps an infinitesimal deformation $f \in \mathcal{C}^\infty(D)$ of a curve $a \in \mathcal{S}_1$ to its L^2-norm, i.e. it is defined by

$$|f|^2_{L^2,a} := \int_D f(\tau)^2 |a'(\tau)| \, d\tau \,. \tag{38}$$

In [15], it is proven that the distance with respect to the above energy between two arbitrary shapes always vanishes and that shortest paths do not exist in general. The authors propose to regularize (38) by the curvature κ_a of a and introduce

$$|f|^2_{L^2_\alpha,a} := \int_D (1 + \alpha\kappa_a(\tau))f(\tau)^2|a'(\tau)|\,d\tau\,. \qquad (39)$$

The parameter $\alpha > 0$ controls the influence of the curvature term. Positive lower bounds for the distance between two different shapes with respect to this energy exist [16].

In our experiments we compare the elastic deformation distance to the distances defined by (38) and (39). Note that the phenomenon of vanishing distances in case of the L^2-norm is due to the infinite dimension of $\mathcal{S}_n$. In the finite dimensional setting of discrete paths of B-spline curves, we can still compute distances with respect to (38).

The example in Figure 5 concerns a beam-like shape bent to the left. Again, the regularized L^2-norm on the left tries to minimize the boundary length weighted by the curvature of the intermediate shapes. The elastic deformation energy deforms the beam such that the required deformation energy is minimal which results in the bottom path.

In the last example we deformed a bone-like shape as illustrated in Figure 6. The shape of the two ends of the straight and the bent bone are exactly the same only their relative position varies and the connecting bar in the middle is deformed. For the (regularized) L^2-norm the details at the ends vanish during the deformation while the elastic deformation energy is able to preserve them.

Finally we want to point out that computation of shortest paths – or geodesics – in general is a difficult problem and that the results in this paper are mostly intended to demonstrate the elastic deformation energy in comparison to other shape metrics. The approach presented here worked well for the examples at hand but is far from being an universal strategy to compute the elastic deformation distance between arbitrary shapes. More complex shapes would most probably require finer discretizations both in space and time. This however renders the numerical computation of the gradient of E_d very expensive as it involves numerous evaluations of the elastic deformation energy.

Also the linear interpolation (37) of the control points is not necessarily an appropriate initial value in every situation and might lead to convergence to (wrong) local minima. Moreover, the presented approach works only for start and end shapes with the same number of control points.
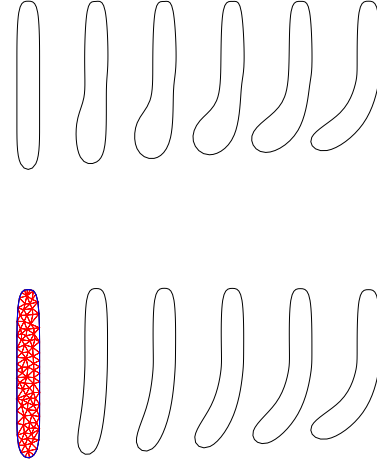

Fig. 5 Shortest paths connecting a bent, beam-like shape with respect to the regularized L^2-norm with $\alpha = 0.0001$ (*top*) and the elastic deformation energy (*bottom*).
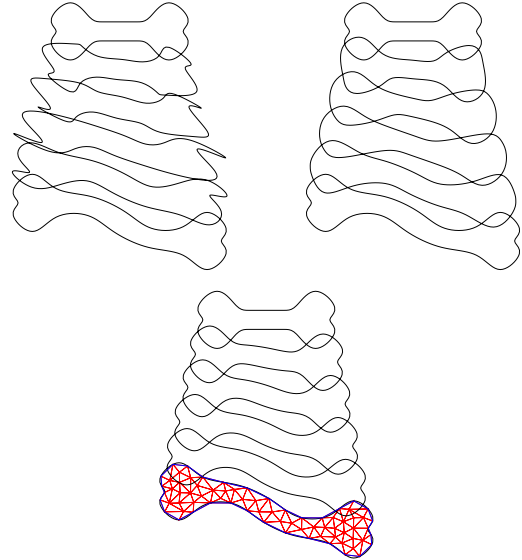

Fig. 6 Shortest paths connecting a deformed bone-like shape with respect to the L^2-norm (*top left*), the regularized L^2-norm with $\alpha = 0.1$ (*top right*) and the elastic deformation energy (*bottom*).

6 Elastic Deformation Shape Modeling

In this section we describe how to use the elastic deformation energy (4) for elastic shape modeling in 3D. Given boundary conditions for the deformation of a 3D object represented by a tetrahedral mesh, we want to obtain a sequence of deformed objects which constitute a realistic animation of elastically deformable models. More specific, we are given a (possibly time-dependent) velocity field which prescribes the infinitesimal defor-

mation of a shape on parts of its boundary. The task is to find the deformation of the remaining part of the shape such that the elastic energy of the global deformation is minimal.

This problem is discretized forward in time. At a fixed time the infinitesimal deformation of the shape which minimizes the elastic deformation energy subject to the prescribed boundary conditions is computed. Then we move the shape according to this deformation multiplied by a small time step. Iterating this process leads to a natural deformation of the shape which is controlled by the given boundary deformations. Note that the results turned out to be satisfactory if we prescribe the complete infinitesimal deformations (not just its normal components) on the boundary. This is reflected in the description of the implementation of one time step below.

6.1 Computation of the deformation field in T-spline space

For the elastic shape modeling in 3D, we compute the elastic deformation energy (4) in a smooth *T-spline* [19] space. We chose the approach of Section 3 and consider the metric perturbation of a globally defined deformation field. More specifically, we define the infinitesimal deformation field $\mathbf{u} : \mathbb{R}^3 \to \mathbb{R}^3$. Then $\mathbf{u}$ corresponds to the infinitesimal displacements at the given time. In our case, we model $\mathbf{u}$ using cubic T-spline functions which means that $\mathbf{u}$ is twice continuously differentiable. This way the computation of energy (4) can be discretized without having to triangulate Ω, a task which is usually more complicated in 3D than in 2D.

In order to define T-spline functions for $\mathbf{u}$, a control grid of T-spline control points (also called *T-mesh*, cf. Figure 7, *top right*) is constructed in the function domain. The distribution of the T-spline control points is adapted to the geometry of the deformable objects, which leads to a compact representation of $\mathbf{u}$. If $K > 0$ is the number of basis functions on the T-mesh, the infinitesimal deformation $\mathbf{u}$ of the function domain is a linear combination of the vectors of the T-spline control points $c^k = (c_1^k, c_2^k, c_3^k)^t \in \mathbb{R}^3$, $1 \leq k \leq K$, and the vectors of the T-spline basis functions $(b_k)_{1 \leq k \leq K}$ (refer to [19] and [22] for more details):

$$\mathbf{u} = \sum_{k=1}^{K} b_k c^k \,. \tag{40}$$

Once the T-mesh is fixed during the deformation, then $\mathbf{u}$ is completely determined by the coefficients $(c^k)_{1 \leq k \leq K}$.

Let $\mathbf{f} \in H^{1/2}(\Gamma)^3$ be the desired infinitesimal deformation on the boundary. Then the elastic energy of $\mathbf{f}$

is defined by (cf. (9))

$$|\mathbf{f}|_{e,a}^2 = \inf_{\substack{c \in \mathbb{R}^{3K} \\ \text{Tr } \mathbf{u} = \mathbf{f}}} E(\mathbf{u}) \,, \tag{41}$$

where $\mathbf{u}$ is computed from c as in (40). In order to solve the above constrained optimization problem in the T-spline space, we use a penalty method to compute the T-spline control points, i.e.

$$c = \operatorname*{argmin}_{c \in \mathbb{R}^{3K}} (E(\mathbf{u}) + F(\mathbf{u})) \,, \tag{42}$$

where

$$F(\mathbf{u}) = \omega \int_{\Gamma} |\operatorname{Tr} \mathbf{u} - \mathbf{f}|^2 \, dx \tag{43}$$

is the penalty function for the boundary constraint, with a large positive weight $\omega > 0$. Since $\mathbf{u}$ is a linear function of c and (41) is quadratic in $\mathbf{u}$, the T-spline control points c can be computed by solving a sparse linear system of equations. The displacement field $\mathbf{u}$ is then obtained by (40).

6.2 Numerical results

We present two examples to illustrate the effectiveness of elastic shape modeling. Again we chose $\mu = 2$ and $\lambda = 0$ in (4) when computing the elastic energy $E(\mathbf{u})$. Numerical integration is used to evaluate both $E(\mathbf{u})$ and the penalty function $F(\mathbf{u})$. The penalty weight is set to be $\omega = 10,000$. Both examples are concerned with a rectangular beam which is deformed according to two different velocity distributions.

In the first example we bend the beam as illustrated in Figure 7. The center node and the nodes at the faces of the beam correspond to the boundary Γ where the deformation of the beam is prescribed. The center of the beam is fixed and the nodes at its ends are moved along a circle perpendicular to the Z-axis.

In the second example we twist the rectangular beam about the X-axis. The initial shape of the object and its deformation are illustrated in Figure 8. During the deformation the faces of the beam are rotated in opposite direction about the principal axis of the beam.

7 Conclusion and Outlook

We introduced the elastic deformation energy (8) of infinitesimal deformations of shapes based on the elastic energy of an isotropic material. The energy is invariant to Euclidean transformations and applies to 1- and 2-dimensional shapes. In contrast to previously proposed metrics on shape manifolds it considers the interior of
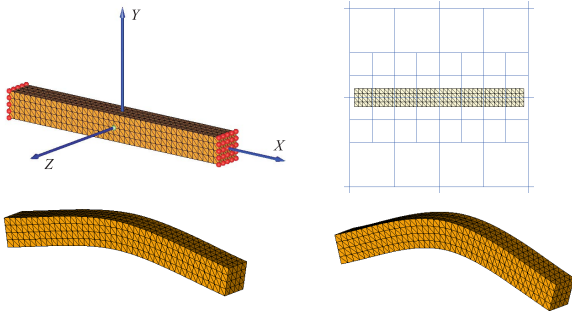
Fig. 7 *Top left*: The initial shape. The deformation of the beam is prescribed at its center and the *red* nodes at its endpoints. The center point is kept fixed, while the ends are moved down along the circle perpendicular to the Z-axis (in the X-Y-plane). *Top right*: The coarse, *blue* grid is the T-spline control grid (T-mesh), which is adapted to the geometry of the beam model depicted by the fine, *yellow* mesh. *Bottom*: The deformed beam at two times.
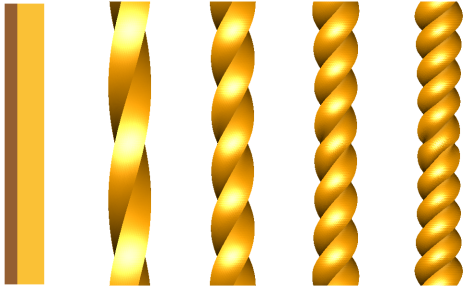

Fig. 8 The initial shape is shown on the *far left*. The deformation of the beam is prescribed at the faces at the ends of the beam which correspond to the *red* nodes in Figure 7, *top left*. The faces are rotated in opposite direction about the principal axis of the beam. The remaining part of the beam deforms accordingly as shown on the remaining images.

the shape instead of only the shape boundary. Thus, it is naturally defined for multiply connected shapes. We proved existence and uniqueness of minimizers in the variational formulation (8) of the elastic deformation energy.

This energy then induces the elastic deformation distance (12). In Section 5 we presented a finite element scheme to compute the elastic deformation energy. Moreover, shortest paths with respect to the elastic deformation distance which connect planar B-spline shapes were exemplarily computed. The use of the elastic deformation energy for shape modeling in space was illustrated in Section 6.

From the theoretic point of view several open questions remain. As mentioned in Remark 7 we are not able to show that $d(a, b) > 0$ if $a \neq b$ (modulo Euclidean transformations). This is due to the fact that we can not give suitable estimates for the dependence of the constant C (*Korn's constant*) in Korn's inequality (18) on the domain Ω. Moreover the existence of geodesics,

i.e. the existence of minimizers of $L(\gamma)$ in (12), is an open problem.

Our approach allows for general topologies of shapes but it requires the topology to stay the same during the evolution. However, if parts of shapes are torn apart or merged together during their deformation, the shape topology changes. To handle such cases the elastic deformation energy has to be adapted in a suitable way.

Finally, for a quantitative analysis of the proposed shape distance, an efficient way to compute shortest paths between shapes is necessary. In contrast to the approach in Section 5, it should be independent of the shape parameterization and robust enough to compare arbitrary shapes. For this purpose the implementation of the shape modeling problem in Section 6 could serve as a reference. It is implicit, i.e. it does not depend on the representation of the shape.

References

1. R. A. Adams. *Sobolev Spaces*. Academic Press, New York-San Francisco-London, 1975.
2. G. Allaire, F. de Gournay, F. Jouve, and A.-M. Toader. Structural optimization using sensitivity analysis and a level-set method. *Journal of Computational Physics*, 194(1):363–393, 2004.
3. W. M. Boothby. *An Introduction to Differentiable Manifolds and Riemannian Geometry*, volume 63 of *Pure and Applied Mathematics*. Academic Press, New York, 1975.
4. G. Charpiat, O. Faugeras, and R. Keriven. Approximations of shape metrics and application to shape warping and empirical shape statistics. *Foundations of Computational Mathematics*, 5(1):1–58, 2005.
5. G. Charpiat, P. Maurel, J.-P. Pons, R. Keriven, and O. Faugeras. Generalized gradients: Priors on minimization flows. *International Journal of Computer Vision*, 73(3):325–344, 2007.
6. P. G. Ciarlet. *Mathematical Elasticity, Volume I: Three-Dimensional Elasticity*. North-Holland, 1988.
7. P. G. Ciarlet and P. Ciarlet Jr. Another approach to linearized elasticity and Korn's inequality. *Comptes rendus de l'Académie des sciences*, I(339):307–312, 2004.
8. S. L. Keeling. Generalized rigid and generalized affine image registration and interpolation by geometric multigrid. *Journal of Mathematical Imaging and Vision*, 29(2–3):163–183, 2007.
9. S. L. Keeling and W. Ring. Medical image registration and interpolation by optical flow with maximal rigidity. *Journal of Mathematical Imaging and Vision*, 23(1):47–65, 2005.
10. D. G. Kendall. Shape manifolds, procrustean metrics, and complex projective spaces. *Bulletin of the London Mathematical Society*, 16(2):81–121, 1984.
11. M. Kilian, N. J. Mitra, and H. Pottmann. Geometric modeling in shape space. *ACM Transactions on Graphics*, 26(3):1–8, 2007.

12. E. Klassen, A. Srivastava, M. Mio, and S.H. Joshi. Analysis of planar shapes using geodesic paths on shape spaces. *Pattern Analysis and Machine Intelligence, IEEE Transactions on*, 26(3):372–383, Mar 2004.

13. S. Lang. *Fundamentals of Differential Geometry*. Springer, New York Berlin Heidelberg, 1999.

14. D. C. Liu and J. Nocedal. On the limited memory BFGS method for large scale optimization. *Mathematical Programming B*, 45(3):503–528, 1989.

15. P. W. Michor and D. B. Mumford. Vanishing geodesic distance on spaces of submanifolds and diffeomorphisms. *Documenta Mathematica*, 10:217–245, 2005.

16. P. W. Michor and D. B. Mumford. Riemannian geometries on spaces of plane curves. *Journal of the European Mathematical Society*, 8(1):1–48, 2006.

17. M. I. Miller and L. Younes. Group actions, homeomorphisms, and matching: A general framework. *International Journal of Computer Vision*, 41(1–2):61–84, 2001.

18. W. Mio, A. Srivastava, and S. Joshi. On shape of plane elastic curves. *International Journal of Computer Vision*, 73(3):307–324, 2007.

19. T. W. Sederberg, J. Zheng, A. Bakenov, and A. Nasri. T-splines and T-NURCCs. *ACM Transactions on Graphics*, 22(3):477–484, 2003.

20. G. Sundaramoorthi, A. Yezzi, and A. Mennucci. Sobolev active contours. *International Journal of Computer Vision*, 73(3):345–366, 2007.

21. H. A. van der Vorst. Bi-CGSTAB: A fast and smoothly converging variant of Bi-CG for the solution of nonsymmetric linear systems. *SIAM Journal on Scientific Computing*, 13(2):631–644, 1992.

22. H. Yang, M. Fuchs, B. Jüttler, and O. Scherzer. Evolution of T-spline level sets with distance field constraints for geometry reconstruction and image segmentation. In *IEEE International Conference on Shape Modeling and Applications 2006 (SMI'06)*, pages 247–252, Los Alamitos, CA, USA, 2006. IEEE Computer Society.

23. A. Yezzi and A. Mennucci. Metrics in the space of curves, 2004.

24. K. Yosida. *Functional Analysis*. Springer Verlag, 1965.

25. L. Younes. Computable elastic distances between shapes. *SIAM J. Appl. Math.*, 58(2):565–586, 1998.

26. J.-P. Zolésio. Control of moving domains, shape stabilization and variational tube formulations. *International Series of Numerical Mathematics*, 155:329–382, 2007.